water

MDPI

Article

Potential of Single-Cell Protein as Novel Biosorbents for the Removal of Heavy Metals from Seawater

Chiara Maraviglia *, Silvio Matassa *, Alessandra Cesaro and Francesco Pirozzi

Department of Civil, Architectural and Environmental Engineering, University of Naples Federico II, Via Claudio 21, 80125 Naples, Italy; alessandra.cesaro@unina.it (A.C.); francesco.pirozzi@unina.it (F.P.)
* Correspondence: chiara.maraviglia@unina.it (C.M.); silvio.matassa@unina.it (S.M.)

Abstract

This study aimed to explore innovative sorbent materials for the remediation of contaminated marine environments, with a focus on metal removal from seawater. Adsorption tests were carried out to evaluate the performance of single-cell proteins (SCPs), a protein-rich biomass derived from industrial by-products, in comparison with commercial activated carbon (AC). Given the increasing need for sustainable and effective approaches in sediment remediation and water treatment, identifying alternatives to conventional sorbents is of particular relevance. Results showed that SCPs exhibited higher affinity for Cr than for Zn, while multi-metal solutions improved adsorption, suggesting synergistic interactions possibly linked to surface charge effects and ternary complex formation. Importantly, SCPs demonstrated competitive and, in some cases, superior performance compared to AC, highlighting their potential as an innovative and sustainable material. Moreover, when the absorbent materials were combined, SCP and AC mixes outperformed both the individual adsorbents and the expected additive efficiencies, achieving significantly higher removal yields for both metals, particularly at low concentrations. Overall, these findings suggest that SCPs, alone or in combination with AC, represent a promising strategy for the removal of heavy metals from marine systems, offering new opportunities for the treatment of contaminated sediments and seawater.

Keywords: single-cell protein; adsorption; heavy metals; remediation; biosorbent

check for updates

Academic Editor: Laura Bulgariu

Received: 8 October 2025
Revised: 5 November 2025
Accepted: 12 November 2025
Published: 14 November 2025

Citation: Maraviglia, C.; Matassa, S.; Cesaro, A.; Pirozzi, F. Potential of Single-Cell Protein as Novel Biosorbents for the Removal of Heavy Metals from Seawater. *Water* **2025**, *17*, 3253. https://doi.org/10.3390/w17223253

Copyright: © 2025 by the authors. Licensee MDPI, Basel, Switzerland. This article is an open access article distributed under the terms and conditions of the Creative Commons Attribution (CC BY) license (https://creativecommons.org/licenses/by/4.0/).

1. Introduction

The contamination of marine environments with heavy metals poses significant environmental and health challenges. These metals, often released from anthropogenic sources near the land surface, can accumulate in marine organisms. This accumulation, in turn, may cause adverse effects on both aquatic life and human health, through direct exposure as well as indirectly, via the food chain [1–3].

After being released into the water environment, soluble heavy metals undergo immobilization and deposition on sediments through mechanisms like adsorption by ion exchange, coagulation with dissolved or suspended species and precipitation as insoluble compounds. The salinity of seawater promotes suspended particle aggregation, accelerating heavy metals sedimentation. As a result, sediments act as reservoirs, adsorbing, accumulating, and, once the environmental or physicochemical conditions change (e.g., pH, Eh, and dissolved oxygen, etc.), potentially releasing heavy metals into surrounding marine water [3,4].

Consequently, developing effective remediation strategies for contaminated sediments is essential to preserve the marine environment.

Sediment remediation techniques can be broadly classified into ex situ and in situ processes. The former involves dredging contaminated sediments and treating them through chemical, physical, or biological processes in specialized reactors. While this approach effectively removes mobile metals, it is costly and can disrupt sediment structure and ecosystem, limiting its large-scale application. On the other hand, in situ remediation primarily focuses on stabilizing heavy metals within the sediment by enhancing their sorption, precipitation, or complexation. These methods are cost-effective, as they do not require sediment removal, but they do not reduce the total metal content and, consequently, under certain conditions, immobilized metals may be remobilized into the water [5]. The main advantage of in situ methods is their simpler implementation, requiring only the addition of amendments to the sediment.

Various in situ remediation techniques have been developed for the treatment of contaminated sediments, each characterized by specific mechanisms of action, advantages, and limitations. Physico-chemical methods, such as solidification/stabilization and sediment flushing, enable contaminant immobilization or facilitate metal recovery. However, their effectiveness may be constrained by factors including sediment depth, heterogeneity, and potential alterations in the physico-chemical properties of the sediments [6]. Electrokinetic separation is a physical technique, which offers operational simplicity and minimal by-product generation, with the added benefit of potential metal recovery. Nevertheless, its performance may be significantly influenced by pH fluctuations, sediment microstructure, and the requirement for additional treatment steps to achieve satisfactory removal of heavy metals [7,8]. Bioremediation represents a low-impact and straightforward biological alternative, although its applicability is typically limited to low-risk sites due to slower kinetics and a higher sensitivity to climatic and geological conditions [9]. Capping and active capping are widely adopted for their cost-effectiveness and environmental compatibility. These approaches are still associated with several technical limitations, including the loss of cap integrity under high hydrodynamic conditions, risk of contaminant breakthrough, and unsuitability in shallow or ecologically sensitive environments [10].

Further, the reactive materials used in the active capping aim to prevent contaminant remobilization not only via physical sequestration—as in conventional capping—but also via adsorption or degradation processes. These processes target both dissolved and weakly adsorbed contaminants, which are released in the aqueous phase and subsequently transferred onto the adsorbent. The possibility of relying on such mechanisms allows for a reduction in the capping layer thickness. Nonetheless, the long-term stability of the active capping may represent a challenge, especially in the marine environment, where several factors may account for the remobilization of the adsorbed contaminant. In this regard, although the recovery of the capping material should be considered, the type of reactive material used may play a role in determining the overall sustainability of this technique, as highlighted by Todaro et al. [11].

Several recent studies have explored the use of waste-derived materials for remediation by active capping of metal-contaminated sediments. This approach not only addresses the issue of waste management circularity but also provides a sustainable solution for pollutant removal.

Industrial slags, for instance, have been widely explored due to their alkaline nature and ability to immobilize metals. In particular, Park et al. [12] demonstrated that steel slag applied as a capping material over artificially contaminated sediments in saline conditions was highly effective in preventing the release of several heavy metals into the overlying water. Similarly, Kutuniva et al. [13] assessed alkali-activated blast furnace slag as a

sediment amendment, showing that it reduced the mobility of multiple contaminants in non-saline water, although its efficiency varied among different metals, with some (e.g., Cr) remaining less effectively immobilized. These studies underline the potential of industrial by-products for sediment remediation, but also highlight challenges related to their performance across a wide spectrum of contaminants and environmental conditions.

More recently, biochar has gained attention as a capping material, particularly due to its origin from renewable feedstocks. For example, Wang et al. [14] tested biochar derived from Enteromorpha under saline conditions, reporting removal efficiencies for Pb and Cd that increased with the applied layer thickness. Despite these promising results, performance remained partial and dependent on experimental conditions, pointing to the need for more efficient and adaptable sorbent systems.

Among non-conventional absorbents which may still be produced from waste substrates, proteins offer a series of interesting properties. Due to their structure, proteins can work as universal molecular adhesives, as they are highly effective in binding a broad range of contaminants in water and making them an ideal and sustainable material for this purpose [15]. For instance, the complex chemistry of whey proteins determines their natural affinity to heavy metals ions [16]. In this context, single-cell proteins (SCPs) hold a great potential. They consist of microbial biomass or protein extracts derived from microorganisms such as bacteria, yeasts, fungi, and microalgae that contain more than 30% protein in their biomass [17]. The production of SCPs using low-cost waste materials from the food and beverage industries, as well as directly from agricultural and forestry resources, is increasingly being explored [17]. This approach utilizes waste substrates such as sugarcane bagasse [18], brewery spent grains, hemicellulose hydrolysate [19], whey [20,21], and other common food industry by-products, including orange and potato residues, molasses, and malt spent rootlets [19], offering a sustainable and cost-effective solution for SCP production.

Previous studies have provided valuable insights into the adsorption performance of proteins and protein-based materials for the removal of heavy metal ions. In particular, Pomastowski et al. [22] showed that casein can effectively adsorb zinc from aqueous solution, while Buszewski et al. [23] confirmed the potential of β-lactoglobulin for Zn removal. For chromium, Peydayesh et al. [24] and Ramírez-Rodríguez et al. [25] reported that protein fibrils obtained from whey proteins were able to retain significant amounts of the contaminant. Although these results are encouraging, most of the existing studies focus on isolated proteins or protein fibrils, tested under controlled laboratory conditions, typically in freshwater and with relatively simple contaminant matrices.

All these studies were carried out in single metal water solutions, as they mainly aimed to propose the use of those novel adsorbents for the treatment of contaminated water. Conversely, the potential of protein-based adsorbent for heavy metal adsorption in seawater has not been evaluated yet.

Taken together, these findings emphasize both the potential and the limitations of current approaches. Industrial by-products such as slags may be efficient in some cases but face challenges in terms of selectivity and long-term stability, while biochar offers versatility but often only achieves partial immobilization under saline conditions. Protein-based adsorbents show excellent affinity for specific metals but have so far been studied mainly in purified forms and not as part of complex biomasses. This leaves an open research space for the development of protein-rich, waste-derived sorbents, such as microbial single-cell proteins, tested in realistic saline environments and under multi-contamination scenarios. By addressing these gaps, such materials could simultaneously advance sustainable waste valorization and provide effective solutions for the remediation of contaminated marine systems.

Moreover, seawater presents a unique and complex matrix, characterized by high salinity and the presence of competing ions [26]. These factors can significantly influence the adsorption behavior of heavy metals mechanism [27], necessitating a thorough investigation to assess the performance of the adsorbent material under marine conditions.

This study explores the potential use of SCPs as novel adsorbent materials for the development of active capping systems that aim to remediate metal-contaminated marine sediments. To this end, zinc and chromium were selected as target contaminants for their properties and high occurrence in real contamination scenarios. More specifically, the former is one of the most transportable and bioavailable heavy metals [28], whereas the latter is known for its high toxicity and carcinogenicity [29]. Batch adsorption experiments were carried out in synthetic seawater contaminated with selected concentrations of zinc and chromium, tested both individually and in combination. These conditions were chosen to simulate the interaction between the adsorbent and dissolved contaminants. This aspect is particularly relevant since active capping technologies are designed to act on pollutants present in the porewater of sediments [30]. The performance of SCPs as adsorbent was compared to that of commercial activated carbon (AC), due to its widespread use and established performance in remediation treatments, providing a suitable benchmark to assess the adsorption efficiency of SCPs. Additionally, different combinations of SCPs and AC were also tested to evaluate potential synergistic effects and to explore the feasibility of using mixed formulations.

2. Materials and Methods

2.1. Solutions and Adsorbents

Single metal solutions were prepared and added to synthetic seawater to run the adsorption tests. To this end, zinc chloride $ZnCl_2$ (PanReach AppliChem, Barcelona, Spain) and potassium dichromate $K_2Cr_2O_7$ (Carlo Erba, Cornaredo, Italy) were first dissolved in deionized water to prepare stock metal solutions (1200 mg/L). Synthetic seawater at 38 psu of salinity was prepared by dissolving 32 gr of Sea Salt (Aquaforest ®, Brzesko, Poland) per liter of demineralized water. The salinity level selected for this study corresponds to the average salinity of the Mediterranean Sea [31] that, being a semi-enclosed basin, exhibits higher salinity levels compared to many open marine environments [32]. This characteristic makes it a relevant model for testing adsorbent materials under challenging conditions, where high salinity could affect their performance.

Table 1 reports the concentrations of the major ions present in the synthetic seawater used in this study.

Table 1. Concentration of major ions in synthetic seawater.

Ion	Concentration [g/L]
Cl^-	14.864 ± 0.271
NO_3^-	0.227 ± 0.114
SO_4^{2-}	2.07 ± 0.112

The pH of the synthetic seawater after preparation was 8.064 ± 0.004.

The metal solutions used for the adsorption tests were prepared by diluting the stock solutions in the synthetic seawater to reach predetermined concentrations of 5, 10, 12.5, 25, 37.5, 50, 75, 100, 150 and 300 mg/L, with the salinity variation considered negligible as the addition of up to 3% by volume of the stock in deionized water would result in only minor salinity variations.

Commercially available AC and dried SCP powder were used as adsorbents. The commercial granular AC used in this study was characterized by a particle size ranging from 0.125 to 2 mm. The SCPs used for this study were obtained from previous experiments investigating their production during the treatment of cheese whey [21]. In particular, they were produced through an innovative process that simultaneously treats excess cheese whey and recovers nitrogen from anaerobic digestate. In this process, ammonia stripped from the digestate is recovered as ammonium in the acidic whey and subsequently upcycled into SCPs through a consortium of yeasts and bacteria. The available SCP powder was primarily composed of proteins, accounting for about 75% of their dry weight. The remaining fraction consisted mainly of carbohydrates, with minor contents of lipids and ash.

2.2. Adsorption Tests

For each test, 400 mg of AC or SCP were added to 40 mL of the heavy metal solutions, resulting in a concentration of 10 g/L of adsorbent, in 50 mL polypropylene falcon tubes. The tubes were sealed with Parafilm and placed on a linear translational shaker to ensure a continuous oscillation at 100 rpm for 48 h at room temperature of 25 ± 1 °C, by adapting the procedure described in Ogata et al. [33]. After the adsorption test, SCPs were separated from the solution by centrifugation at 13,000 rpm for 15 min and filtered with mixed cellulose ester (MCE) syringe filters with a pore size 0.45 µm. In AC samples, instead, the adsorbent was separated from the solution by filtration with MCE syringe filters with pore size of 0.45 µm. Control tests, without adsorbent addition, were carried out as well. All tests were performed in duplicate.

2.2.1. Experimental Conditions

Zn and Cr adsorption capacity of both SCPs and AC was tested in single and binary metal solutions at different concentrations.

Adsorbent capacities at 48 h were determined for each adsorbent in single metal solutions at concentration of 10, 25, 50, 75, 100, 150 and 300 mg/L. For binary solutions, the concentration of Zn and Cr are those reported in Table 2.

Table 2. Concentration of Zn and Cr in binary solutions.

	BinSol1	BinSol2	BinSol3	BinSol4	BinSol5	BinSol6
Zn [mg/L]	5	12.5	25	37.5	50	75
Cr [mg/L]	5	12.5	25	37.5	50	75

Additional adsorption tests were carried out using a mix of the target adsorbents, as given in Table 3.

Table 3. AC and SCP content in MIX1 e MIX2.

	MIX 1	MIX 2
AC content [g/L]	2.5	7.5
SCP content [g/L]	7.5	2.5

MIX1 and MIX2 adsorbent capacities were tested in single metal solutions at either 10 or 50 mg/L as well as in binary solutions, composed of 5 and 25 mg/L of each target metal.

The adsorption capacity under different experimental conditions was referred to the variation in the target metal concentration in solution, as detailed in Section 2.4.

2.2.2. Analytical Setup

The concentration of chlorides, nitrates, and sulfates in synthetic seawater was analyzed using an Ion Chromatograph (Metrohm, Herisau, Switzerland) equipped with an IonPac AS12A anionic column while the pH was determined using a WTW inoLab® Multi 9620 IDS meter (Xylem Analytics, Weilheim, Germany) equipped with a WTW digital pH electrode Sentix® 940. Surface functional groups characterization of dried SCP was carried out by IRSpirit-ZX FTIR spectrophotometer (Shimadzu, Kyoto, Japan).

Target metal concentrations were determined via Varian SpectrAA 50 atomic absorption spectrometer (Agilent, Santa Clara, CA, USA) at the beginning and end of each adsorption test. The measurement was run in duplicate and the results expressed as average values.

2.3. Calculations

The target metal concentration data were used to calculate metal removal efficiencies and the equilibrium metal ion adsorptive quantity.

Heavy metals removal efficiency was calculated as indicated in the following equation (Equation (1))

$$\eta = \frac{(C_{ctrl,e} - C_e)}{C_{ctrl,e}} \cdot 100 \quad (1)$$

where $C_{ctrl,e}$ (mg/L) is the equilibrium target metal ion concentration in the control sample solution at the end of the adsorption test and C_e (mg/L) is the equilibrium target metal ion concentration in the solution at the end of the adsorption test.

Heavy metal loading (q_e, mg/g) onto AC and SCP was calculated using the following equation (Equation (2))

$$q_e = \frac{(C_{ctrl,e} - C_e) \cdot V}{m} \quad (2)$$

where V (L) is the volume of aqueous solution, m (g) is the solid adsorbent mass, $C_{ctrl,e}$ (mg/L) is the equilibrium target metal ion concentration in the control sample solution at the end of the adsorption test and C_e (mg/L) is the equilibrium target metal ion concentration in the solution at the end of the adsorption test.

In both cases $C_{ctrl,e}$ is used instead of the initial target metal ion concentration (C_0) to take into account changes in metal ion concentrations in solution that are not related to the adsorption process.

To assess the speciation of the target metals in synthetic seawater, simulations were performed using Visual MINTEQ (ver 4.07). The simulation was carried out using the chemical composition of the synthetic seawater shown in Table 1 and the pH value measured, in order to replicate the conditions of the experimental setup.

2.4. Adsorption Isotherms

The experimental data for target metals obtained through the adsorption tests were modeled by the isotherm models of Langmuir and Freundlich.

The Langmuir isotherm is defined as follows (Equation (3)):

$$q_e = \frac{Q_{max} K_L C_e}{1 + K_L C_e} \quad (3)$$

where q_e (mg/g) is the adsorption capacity at equilibrium, C_e (mg/L) is the equilibrium metal ion concentration, Q_{max} is the maximal adsorption capacity and K_L is Langmuir constant, that is related to the affinity between the adsorbent the adsorbate [34].

Once modeled, the separation factor (R_L) was evaluated. R_L is a dimensionless constant that indicates the favorability of an adsorption process, defined as follows (Equation (4)):

$$R_L = \frac{1}{1+K_L C_{ctrl,e,max}} \quad (4)$$

where K_L is the Langmuir constant derived from the isotherm model fitting and $C_{ctrl,e,max}$ is the maximum equilibrium target metal ion concentration in the solution of the control sample without adsorbent at the end of the adsorption test.

The nature of the adsorption process is indicated by the separation factor [35]:

- linear ($R_L = 1$);
- irreversible ($R_L = 0$);
- favorable ($0 < R_L < 1$);
- unfavorable ($R_L > 1$).

The Langmuir model assumes monolayer adsorption with a uniform distribution of adsorption sites and energies, and no interactions between the adsorbed molecules or ions [36]. Despite the irregular shapes and non-uniform surfaces of adsorbent materials (such as AC), adsorption can still be described by the Langmuir isotherm [37].

The Freundlich isotherm is defined as follows (Equation (5)):

$$q_e = K_f C_e^{1/n} \quad (5)$$

where q_e (mg/g) is the sorption capacity at equilibrium, C_e (mg/L) is the equilibrium metal ion concentration, and K_f and n are constants.

The Freundlich model accounts for lateral interactions between the adsorbed molecules or ions and reflects the energetic distribution of adsorption sites, as well as the diverse nature of the adsorbed metal ions, whether free or in hydrolyzed forms [36]. In most studies, the Freundlich isotherm is used to represent multilayer adsorption on heterogeneous surfaces [38,39]. In the equation reported above, the constants K_f and n, respectively, refer to the adsorption capacity and its intensity [40]. If $1/n = 1$, the adsorption is linear, homogenous and there is no interaction between the adsorbed species, when $1/n < 1$ the adsorption process is considered favorable, while $1/n > 1$ the adsorption is unfavorable [41].

The modeling of experimental data was performed with OriginPro 2024b software.

To improve model fitting and enhance the physical interpretation of the adsorption process, a sensitivity analysis on model parameters was performed to identify and exclude outlier data points. This iterative approach involved progressively refining the dataset by removing points that significantly deviated from the expected trend, while preserving a minimum of five data points for the modeling. The final models consistently achieved a correlation coefficient (R^2) greater than 0.90.

3. Results and Discussion

3.1. Simulation of Metal Speciation

The simulation performed using the chemical composition of the synthetic seawater reported in Table 4 at the measured pH value, and considering each target metal at a concentration of 150 mg/L, both individually and in combination, indicated that Cr and Zn primarily exist as a dissolved polyatomic anion, chromate (CrO_4^{2-}), and a free cation (Zn^{2+}), respectively. This suggests that the two metals may undergo different adsorption pathways, reflecting their distinct ionic forms in solution. In Table 4, the input and output element concentrations of the simulations are reported.

Table 4. Simulation input parameters and concentrations (left), output Zn and Cr species from bigger to smaller (right).

Input Parameters	
Components	**Concentration [mg/L]**
Cl^-	14,864
$N(NO_3^-)$	227
SO_4^{2-}	2070
Mg^{2+}	1605
Ca^{2+}	477
K^+	567
H^+	0
Zn^{2+}	0
CrO_4^{2-}	0
Na^+	8066
Finite Solids	**Amount (mol/l)**
$ZnCl_2$(s)	2.29
$K_2Cr_2O_7$(s)	1.44
Fixed species	Log activity
H^+	−8
Output Concentrations	
Cr^- Species	**Concentration (mg/L)**
CrO_4^{2-}	0.671
$Cr_2O_7^{2-}$	0.110
$KCrO_4^-$	0.104
$NaCrO_4^-$	0.047
$KCr_2O_7^-$	0.033
$CaCrO_4$ (aq)	0.009
$HCrO_4^-$	0.002
CrO_3Cl^-	1.1×10^{-8}
$CrO_3SO_4^{2-}$	2.7×10^{-9}
H_2CrO_4 (aq)	9.3×10^{-12}
Zn^- Species	**Concentration (mg/L)**
Zn^{2+}	0.720
$ZnCl_4^{2-}$	0.670
$ZnCl^+$	0.493
$ZnCl_3^-$	0.203
$ZnCl_2$ (aq)	0.190
$ZnSO_4$ (aq)	0.012
Zn_2OH^{3+}	0.001
$Zn(SO_4)_2^{2-}$	0.001
$ZnOH^+$	1.2×10^{-4}
$Zn(OH)_2$ (aq)	1.1×10^{-6}
$Zn(OH)_3^-$	4.2×10^{-12}
$Zn(OH)_4^{2-}$	2.5×10^{-18}

3.2. Characterization of Adsorbent Materials

FT-IR analysis was carried out to identify the main functional groups of SCPs. In Figure 1, the FT-IR spectrum of SCPs is plotted, and Table 5 reports the functional groups and the specific wavelengths at which they were detected.

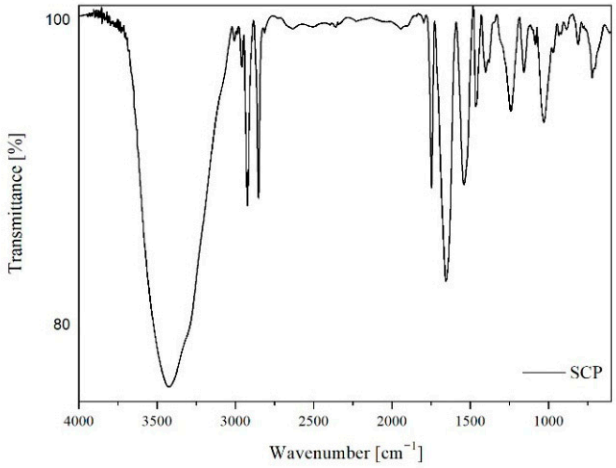

Figure 1. SCP FT-IR spectrum.

Table 5. Functional groups of SCPs.

Wavenumber [cm^{-1}]	Functional Group
3500	O–H stretching vibrations
2925	–C–H (CH_2 groups) stretching vibration
2854	–C–H (CH_3 groups) stretching vibration
2745	C=O stretching of ester or carboxylic acid group
1654	Amide I (C=O and C–N stretching vibrations)
1540	Amide II (N–H bending vibrations, C–N stretching vibrations)
1405	Amide II (COO– stretching vibrations)
1245	Amide III (C–N, N–H bending vibrations)
1027	Amide III (C–O stretching vibrations)
711	N–H bending vibrations

The FT-IR spectra of the two adsorbents highlight their distinct chemical compositions and potential interaction mechanisms with heavy metals. The SCP spectra confirm the presence of key functional groups within the material, specifically hydroxyl, carboxyl and amino groups. These groups are well recognized in the literature as the primary functional sites responsible for complexation with metal ions, playing a crucial role in the adsorption process, as reported in Nong et al. [42].

FT-IR analyses on commercial activated carbons used in different studies [43–45] have identified several common surface functional groups. Among them, hydroxyl groups (–OH), aliphatic, methyl and methylene carbon-hydrogen groups, carbonyl groups (C=O), aromatic structures (C=C), phenolic carbon-oxygen groups and carboxyl functional groups (–COOH) are commonly detected. Based on this FT-IR evidence, it is expected that the interaction of AC with the heavy metals in aqueous solutions should occur with the hydroxyl, carbonyl and carboxyl groups, as previously reported in the literature [46].

3.3. Adsorption Tests

3.3.1. Removal Efficiency of SCPs in Single and Binary Systems

As reported in Figure 2b, the SCPs demonstrated a higher affinity for Cr adsorption than for Zn, as the tests carried out at the lowest metal concentrations resulted in a maximum removal of nearly 60%, in both single and binary solutions. The performance decreased, mostly following a linear trend, reaching around 13% and 18% at 300 mg/L of Cr, in single and binary solutions, respectively. This behavior may be attributed to the saturation of available binding sites on the SCP surface at higher concentrations, which can reduce the effectiveness of adsorption. Similar Cr adsorption yields in single and mixed solutions may reflect either the stronger interaction, compared to Zn, of Cr with functional groups on SCP or a preferential binding mechanism not influenced by the coexisting Zn ions.

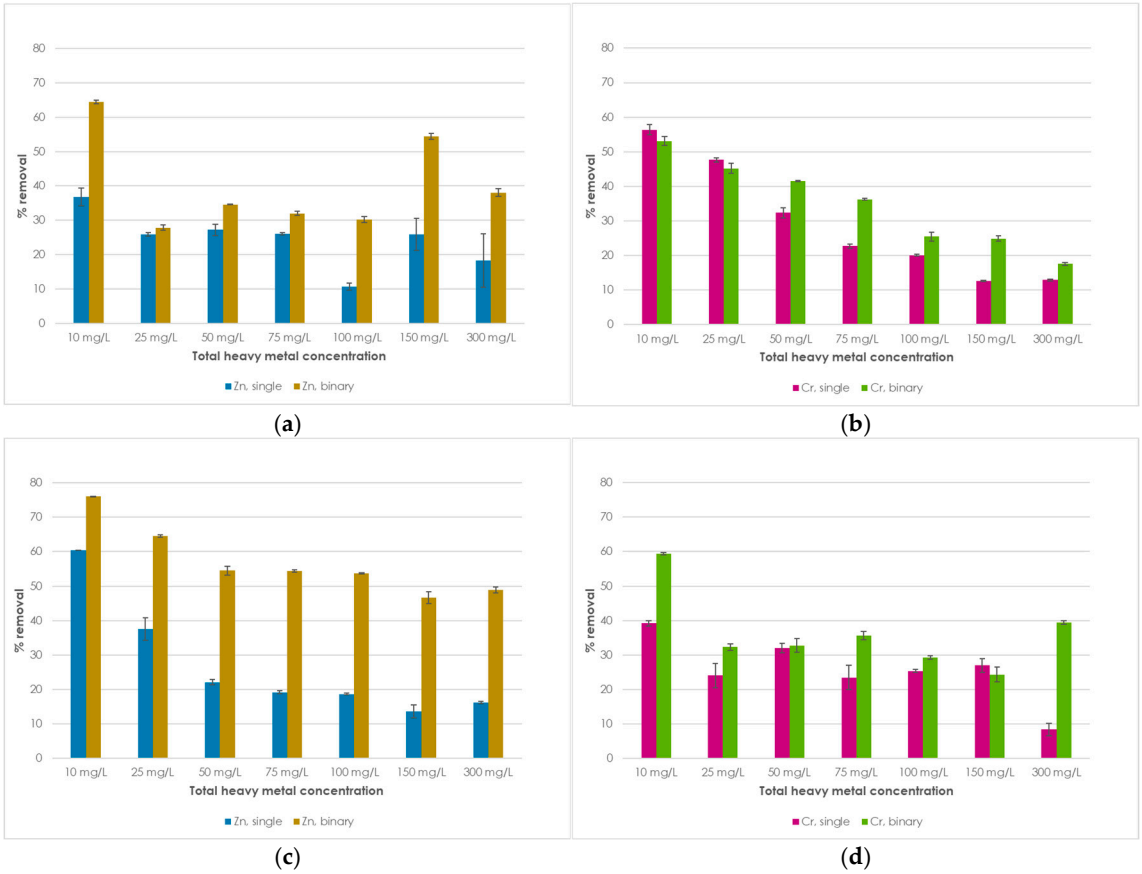

Figure 2. Zn (**a**) and Cr (**b**) removal efficiencies of SCPs in single and binary solutions; Zn (**c**) and Cr (**d**) removal efficiencies of AC in single and binary solutions.

The SCP performed better than the AC, which exhibited a maximum removal efficiency of around 40% at the lowest Cr concentration tested (10 mg/L). Under the most challenging condition of 300 mg/L of Cr, a minimum efficiency of just over 8% was obtained, yet with a non-linear variation in the specific adsorption capacity with the different concentrations tested.

A beneficial effect was observed for Cr adsorption on AC in mixed solutions, as reported in Figure 2d, with removal efficiencies increasing from about 40% to 60% when moving from the higher to the lower concentration tested. This suggests the occurrence of a synergistic effect, possibly due to changes in surface charge distribution that favor the co-adsorption of both Cr and Zn ions.

Zn adsorption on SCP in single solution is plotted in Figure 2a. The minimum efficiency, observed in tests at the highest metal concentration, was just over 18%, while the maximum efficiency at 10 mg/L of metal was around 37%. In this case, the performance trend at different metal concentrations does not appear to be linear, suggesting that multiple mechanisms may contribute to Zn adsorption, potentially involving site-specific interactions and/or changes in metal speciation at varying concentrations [47].

As shown in Figure 2c, Zn removal by adsorption onto AC varies between 13% and 60% in single solutions. The maximum value of about 60% was reached in tests carried out at 10 mg/L, while efficiency decreased as the concentration in the solution increased, with a minimum value of approximately 13% for tests carried out at 150 mg/L. This trend suggests that the number of available adsorption sites on AC becomes progressively saturated at higher Zn concentrations, limiting the removal efficiency despite the greater availability of contaminants.

An improvement in the material's adsorption performance towards Zn on SCP was observed following the addition of the second metal in the solution. The removal efficiencies of Zn in mixed solutions ranged between 40% and 65%. This enhancement indicates a possible synergistic interaction between the two metals, potentially driven by either anion bridging effects, or the formation of ternary surface complexes, as mentioned in the previous section [48].

As reported in Figure 2b, in the presence of Cr, also Zn adsorption on AC improved compared to tests carried out in single solutions. The removal efficiency ranged from 50% to 76% as the total metal concentration decreased, showing an almost linear trend.

Such a synergistic effect was previously observed also in co-adsorption studies involving anions or cations in water solutions. In particular, Liu et al. [48] reported that oxidized arsenate species As(V), due to their negative charge and dissociative behavior, enhanced the adsorption of Cd(II) through both anion bridging and electrostatic shielding effects. Specifically, deprotonated As(V) acted as a bridge between the positively charged adsorbent surface and Cd(II) cations, effectively reducing electrostatic repulsion and facilitating metal retention. In the same study, a reciprocal enhancement was also observed, where the presence of Cd(II) promoted the adsorption of As(III) via the formation of ternary surface complexes and hydrogen bonding. Similarly, Ren et al. [49] demonstrated that phosphate ions increased the retention of Cu(II) on γ-Al_2O_3, with the effect strongly dependent on phosphate concentration. In this case, phosphate acted as a bridging ligand, stabilizing Cu(II) on the adsorbent surface. These findings suggest that specific anionic species, such as the chromate formed in this study after Cr addition in synthetic seawater (Section 3.1), may play an active role in modulating the adsorption of metal cations, namely zinc. This mechanism could involve bridging interactions, a mechanism that could potentially contribute to the behavior observed in the present study.

3.3.2. Isotherm Modeling for Individual Adsorbents

Figure 3 plots the Langmuir and Freundlich isotherm curves, and in Table 6, the parameters obtained from the modeling of experimental adsorption data for Zn on AC and SCPs in single and mixed solutions are presented.

Regarding the adsorption of Zn on proteins, varying behaviors have been reported in the literature. In both Buszewski et al. [23] and Pomastowski et al. [22], the Q_{max} values for Zn adsorption on β-lactoglobulin and casein, respectively, equal to 104.4 mg/g and 30.05 mg/g, are higher than those obtained in this study. However, this discrepancy may be attributed to differences in the nature and structure of the proteins. The SCPs used in this study are proteins derived from a mixed microbial inoculum, which inherently leads to a heterogeneous composition. By contrast, the proteins commonly reported in the literature

belong to defined single classes, characterized by a defined amino acid composition and known structures.

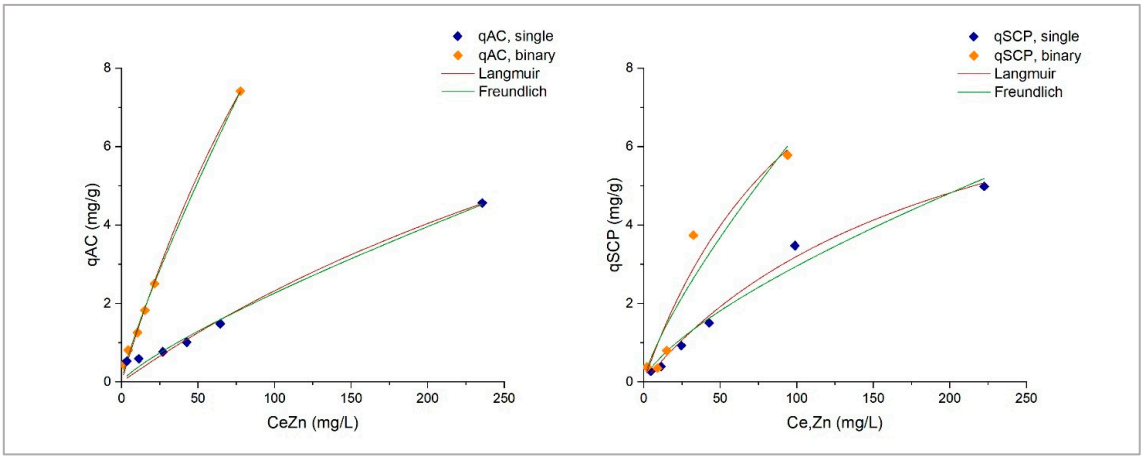

Figure 3. Langmuir and Freundlich isotherms fitted curves of adsorption process of Zn in both AC (**left**) and SCP (**right**).

Table 6. Langmuir and Freundlich parameters of modeled adsorption process of Zn on AC and SCP.

Test Condition	**Langmuir**			**Freundlich**		
	$\mathbf{Q_{max}}$	$\mathbf{K_L}$	$\mathbf{R^2}$	$\mathbf{K_f}$	**n**	$\mathbf{R^2}$
	[mg/g]	**[L/mg]**	**[-]**	**[(mg/g)(L/mg)$^{1/n}$]**	**[-]**	**[-]**
Zn, single, SCP	9.728	0.005	0.991	0.115	1.419	0.975
Zn, binary, SCP	13.31	0.009	0.931	0.176	1.288	0.912
Zn, single, AC	15.51	0.002	0.976	0.055	1.237	0.982
Zn, binary, AC	27.591	0.005	0.996	0.188	1.185	0.998

The Q_{max} value of AC derived from the Langmuir model fitting in a single-metal solution of Zn is consistent with the results reported in previous studies carried out in aqueous systems [36], suggesting that, under the tested conditions, the salinity of the medium did not significantly affect the adsorption performance of AC for Zn.

Zn adsorption on SCPs is better described by the Langmuir isotherm model, indicating a homogeneous process. The adsorption capacity is higher in the presence of Cr in the solution, reaching values of 9.73 and 13.3 mg/g in single and binary solutions, respectively. Under this condition, SCP also shows a higher affinity for Zn, as suggested by the K_L parameter, which is greater in the binary system.

By comparison, the adsorption process of Zn on AC is more consistent with the Freundlich isotherm model, as evidenced by the higher correlation coefficient (R^2) values obtained for both the solutions tested. This suggests a heterogeneous adsorption mechanism with interactions between the adsorbed ions. The K_f parameter is higher in binary solution adsorption, indicating a greater adsorption capacity of AC under these conditions. Conversely, the n coefficient, which relates to the intensity of the adsorption process, is higher in single-metal solutions, suggesting a stronger affinity when no other metals are present.

Table 7 presents the R_L and 1/n coefficient values, calculated from the isotherm parameters obtained through the modeling of experimental data.

Table 7. R_L and 1/n coefficients calculated from Langmuir and Freundlich isotherm parameters for Zn adsorption on AC and SCPs.

Test Condition	R_L	1/n
Zn, single, SCP	0.424	0.705
Zn, binary, SCP	0.423	0.776
Zn, single, AC	0.640	0.808
Zn, binary, AC	0.568	0.844

The coefficient values indicate that the adsorption process is favorable under all tested conditions, as they range between 0 and 1.

Figure 4 and Table 8 present the Langmuir and Freundlich isotherm curves along with the parameters obtained from the modeling of experimental Cr adsorption data on AC and SCPs in both single and binary solutions.

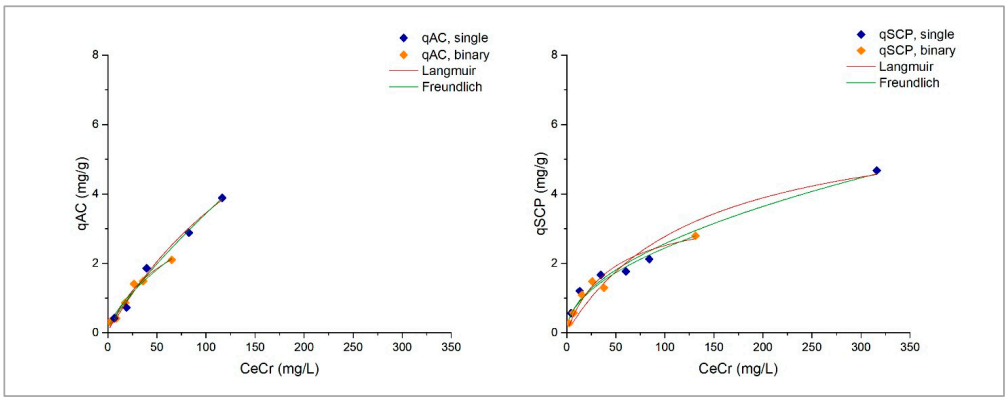

Figure 4. Langmuir and Freundlich isotherms fitted curves of adsorption process of Cr in both AC (**left**) and SCP (**right**).

Table 8. Langmuir and Freundlich parameters of Langmuir and Freundlich parameters of modeled adsorption process of Cr on AC and SCPs.

Test Condition	Langmuir			Freundlich		
	Q_{max}	K_L	R^2	K_f	n	R^2
	[mg/g]	[L/mg]	[-]	$[(mg/g)(L/mg)^{1/n}]$	[-]	[-]
Cr, single, SCP	6.497	0.007	0.916	0.252	1.984	0.978
Cr, binary, SCP	3.623	0.023	0.946	0.249	2.019	0.966
Cr, single, AC	11.066	0.005	0.989	0.089	1.262	0.989
Cr, binary, AC	3.971	0.017	0.972	0.146	1.551	0.967

For what concern the adsorption of Cr on proteins, the results obtained in Peydayesh et al. [24] differ from those of this study, as they report an adsorption capacity that is one order of magnitude higher for amyloid membranes tested by filtering Cr solution at lower concentration (174 ppb) than those tested in this study. This difference may be primarily attributed to the different types of tests carried out, as the adsorption mechanism in a filtration process may differ from that observed in a batch adsorption setup, but also to the different nature of the adsorbent material.

The Q_{max} value obtained from the Langmuir isotherm in the single-metal solution is slightly higher than those reported in previous studies involving Cr adsorption. In Selvi et al. [50], who obtained a Q_{max} of 3.46 mg/g on activated carbon, this discrepancy could be attributed to the different operating conditions, which may have influenced the

adsorption process: lower values of the tested concentration, pH, and contact time were indeed adopted. Conversely, in Di Natale et al. [51], who obtained a Q_{max} of 2.50 mg/g for the adsorption of Cr on granular activated carbon, the main difference lies in the narrower concentration range used in their experiments.

The interpretation of the parameters obtained from the modeling indicates that Cr adsorption on SCPs is better described by the Freundlich isotherm model, indicating a heterogeneous process. In this case, both K_f and n coefficients, related to adsorption capacity and process intensity, respectively, do not show significant variations between single and binary solutions. This suggests that Cr adsorption is neither hindered nor enhanced by the presence of a second metal in solution, in good agreement with the removal efficiency results discussed in the previous paragraph.

By comparison, the adsorption process of Cr on AC is better described by the Langmuir isotherm model, as indicated by the higher correlation coefficients (R^2) compared to the Freundlich model. This suggests a homogeneous process without interactions between the adsorbed ions on the material. The highest Q_{max} value is obtained in single-metal solutions, reaching 11.97 mg/g for the adsorption on AC, while a greater affinity can be inferred in binary solutions, as suggested by the greater K_L values.

Table 9 presents the R_L and 1/n coefficients, calculated from the isotherm parameters obtained through the modeling of experimental data. Also in this case, the coefficients values indicate that the adsorption process is favorable under all the tested conditions.

Table 9. R_L and 1/n coefficients calculated from Langmuir and Freundlich isotherm parameters for Cr adsorption on AC and SCPs.

Test Condition	R_L	1/n
Cr, single, SCP	0.283	0.504
Cr, binary, SCP	0.214	0.495
Cr, single, AC	0.449	0.867
Cr, binary, AC	0.270	0.563

3.3.3. Removal Efficiency in Single Metal Solutions at Different Adsorbent Mix Ratios

To assess any synergistic effects due to the combination of the two adsorbent materials under study, and to further evaluate their potential combined employment in real applications, experimental tests were carried out in single metal solutions using two adsorbent mixes. Figure 5 shows the removal efficiency observed for the target metals in tests carried out on the two mixes.

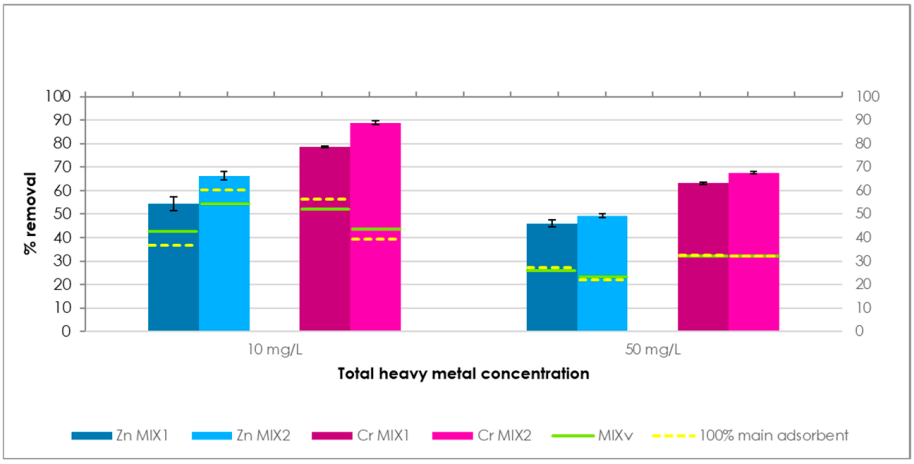

Figure 5. Zn and Cr removal efficiencies of MIX1 and MIX2 in single heavy metal solutions.

The removal efficiencies of Zn and Cr by the two adsorbent mixes (MIX1 and MIX2) were compared to the theoretical efficiency of two virtual mixes (MIX1v and MIX2v), calculated as the weighted average of the efficiencies obtained from the adsorption tests on the two single adsorbents. These virtual efficiencies are represented by the solid line within each bar, while the dashed line indicates the efficiency obtained from the tests on the main adsorbent of each MIX used alone at 100% dosage.

Compared to the results of adsorption tests on SCPs, MIX1, which is primarily composed of SCPs, shows better performance by about 18% for both Zn concentrations tested. This suggests that the addition of a small fraction of AC to SCPs may enhance the availability or diversity of adsorption sites, possibly contributing to a more efficient Zn uptake. When compared with the estimated removal efficiency of the virtual adsorbent mix MIX1v, the actual MIX1 showed a Zn removal efficiency higher by approximately 12% at the initial concentration of 10 mg/L and by about 20% at 50 mg/L.

Zn adsorption yield on MIX2, which is predominantly made up of AC, is similar to that observed with only AC for the Zn concentration of 10 mg/L, indicating that the presence of a minor SCP fraction did not significantly alter the adsorption behavior at lower concentrations. Nonetheless, higher efficiencies of about 27% were observed for tests carried out at 50 mg/L, suggesting a possible beneficial interaction between the two materials at intermediate contaminant levels, potentially due to complementary adsorption mechanisms or improved surface accessibility [52,53]. By comparison, the removal efficiency of the actual MIX2, as opposed to the estimated value of the virtual mix (MIX2v), was higher by about 12% at the lower Zn concentration (10 mg/L) and by approximately 26% at the higher concentration (50 mg/L).

Regarding Cr adsorption on MIX1, the efficiency obtained at low solution concentration (≈78%) was about 27% higher than that of the main single adsorbent (SCP), while it exceeded the estimated value of the virtual mix by about 22%. At the higher Zn concentration (50 mg/L), the efficiency of MIX1 was instead about 30% higher compared with both the single main adsorbent and the virtual mix MIX1v.

Similarly, MIX2 showed a much better response in terms of Cr adsorption yields compared to the removals obtained with only AC and estimated for the virtual adsorbent mix MIX2v. In tests carried out at 10 mg/L of Cr, MIX2 reached removal efficiency values of around 90%, exceeding both the single adsorbent and virtual efficiency by over 45%. For tests carried out at 50 mg/L of Cr in solution, the removal efficiency was around 67%, showing an improvement of about 35% over both reference values.

Overall, the findings suggest that combining SCP and AC in appropriate ratios can lead to synergistic effects, improving the adsorption capacity for both metals beyond what is observed for the individual materials, enhancing their adsorption performance over the expected additive effect.

3.3.4. Removal Efficiency in Binary Metal Solutions at Different Adsorbent Mix Ratios

Finally, tests were carried out to evaluate the adsorptive capacity of the two material mixes described above in binary solutions, and the results are shown in Figure 6.

In the case of adsorption on MIX1, the Zn adsorption yields at the total concentration of both target metals are similar to those obtained in single Zn solutions at the same total metal concentration, suggesting that the presence of Cr did not negatively affect Zn adsorption. When comparing these results with the removal efficiencies on the single main adsorbent (SCP) and the estimated virtual efficiency, the values for the tests carried out at the total target metal concentration of 10 mg/L are, respectively, lower by about 12% and 15%. At the total metal concentration of 50 mg/L, the removal efficiency values are slightly above, by about 8% and 13%.

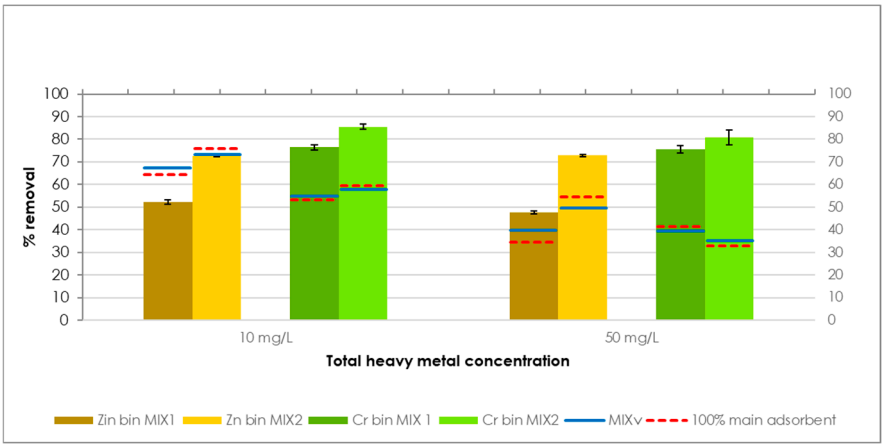

Figure 6. Zn and Cr removal efficiencies of MIX1 and MIX2 in binary heavy metal solutions.

Conversely, a slight improvement in performance for binary solutions is observed in tests carried out with MIX2, achieving removal yields of approximately 73% at both total metal concentration levels. As in the previous case, the removal efficiencies obtained with the main single adsorbent (AC) and those calculated for the virtual mix MIX2v are slightly lower than the values from MIX2 tests at the lower concentration level, whereas they exceed them by 18% and 23%, respectively, at the higher concentration level tested.

Regarding Cr removal efficiencies, they are similar to those obtained in tests on both mixes carried out in Cr solutions at a concentration of 10 mg/L, while the adsorptive performance is slightly higher than that observed in tests carried out at 50 mg/L of Cr. This result could indicate that the coexistence of Zn may have favored Cr retention on the adsorbent surface, possibly through mechanisms such as ternary complex formation or changes in surface charge distribution induced by the co-adsorbed cation [54,55].

When comparing these results with the two reference values, the performance of MIX1 is better by over 22% and 34% with respect to both the virtual and the main adsorbent (SCP) efficiency at the lower and higher total metal concentrations tested. Meanwhile, the adsorption levels on MIX2 are higher by over 26% and 45%, respectively, at the same concentrations.

3.3.5. Adsorbent Capacity Comparison for Mixed Adsorbents

In the following Figure 7, the adsorption capacity of the two tested adsorbent mixes in single and binary solutions at different tested concentrations are presented.

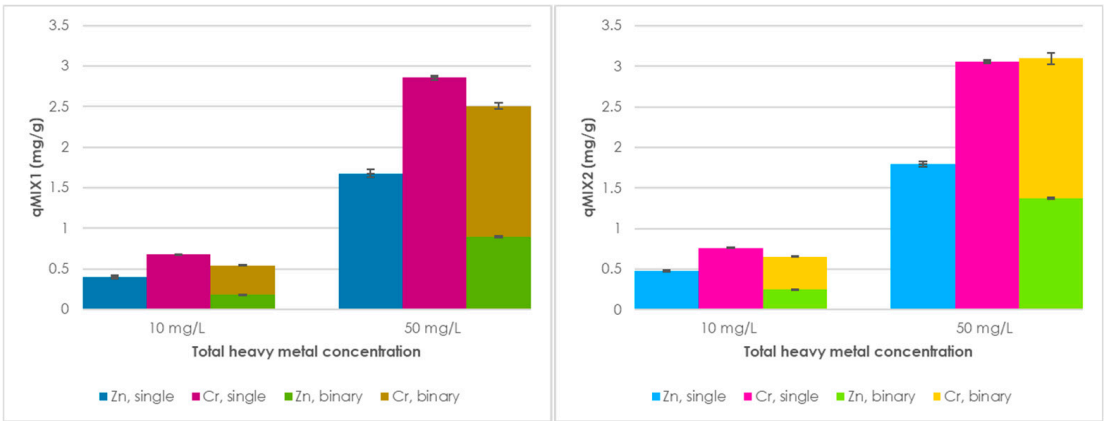

Figure 7. Adsorption capacities of MIX 1 (**left**) and MIX 2 (**right**) at 10 mg/L and 50 mg/L of target metals in both single and binary metal solutions.

As shown in the figure, the adsorption behavior of MIX1 and MIX2 in both single and binary solutions at low total metal concentrations (10 mg/L) appears to be similar. When comparing the adsorption capacity values obtained for each target metal under these conditions, the maximum difference observed is 0.088 mg/g for Cr in single-metal solutions. This evidence suggests that, at this contamination level, the different ratios of the two adsorbent materials do not significantly affect performance, indicating a comparable affinity of the two mixes for both Cr and Zn. This result could reflect a saturation threshold of active sites far from being reached, making the influence of adsorbent composition less relevant at low contaminant levels.

At a higher total metal concentration (50 mg/L), the two mixes continue to show similar adsorption capacities in single-metal solutions, although MIX2 demonstrates a slightly higher performance. This could be attributed to the higher proportion of activated carbon in MIX2, which may offer a greater number of high-affinity binding sites for metal ions at elevated concentrations.

In contrast, in binary-metal solutions at the same total concentration, the adsorption behavior toward Cr remains similar between the two mixes, while a more pronounced difference is observed in Zn adsorption. Specifically, MIX2 shows an increase of approximately 0.48 mg/g in Zn adsorption capacity compared to MIX1. This improvement may suggest a synergistic effect associated with the simultaneous presence of Cr, potentially enhancing Zn retention through cooperative adsorption mechanisms or the formation of bimetallic surface complexes. This hypothesis aligns with previous findings indicating that the presence of certain metal species, such as chromate anions, can facilitate the adsorption of metal cations by acting as bridging ligands or altering the adsorbent surface charge [48].

3.4. Technical Implications and Application Perspectives

The findings of this study highlight both the technical feasibility and the limitations of using SCPs and commercial AC as adsorbent materials for reactive capping applications in contaminated marine environments.

SCPs demonstrated promising adsorption capacities, particularly for Cr, and showed improved performance in binary solutions, suggesting potential synergistic effects in multi-contaminant scenarios. As a bio-based material, SCP aligns with circular economy principles, especially when produced from industrial waste streams. Its biodegradable and low-toxicity nature [56] also represents an advantage for environmental compatibility in long-term capping strategies.

However, multiple technical challenges and research gaps require additional effort. The solubility of SCP in marine water could compromise the physical stability of the capping layer, especially under high-flow conditions. Further research is needed to enhance the structural integrity of SCP-based caps, for instance by incorporating them into composite matrices or applying stabilization treatments [57]. Additionally, variability in SCP composition depending on production conditions may affect adsorption performance [58], thus requiring standardization protocols for potential field applications.

For these reasons, the results presented in this study are valid for the specific type of SCP tested, and further research will be necessary to assess whether similar adsorption performance can be observed for SCP produced through other processes.

Commercial AC, on the other hand, offers robust and consistent adsorption performance across various conditions and showed improved Zn removal in the presence of Cr. Its hydrophobic properties and high surface area make it particularly effective in adsorbing a broad range of organic and inorganic contaminants [59]. Its use in reactive capping has been widely studied and field-tested [12,60] providing a strong basis for technical reliability.

Nonetheless, AC presents some drawbacks, including potential ecological impacts related to its persistence in the environment [61].

In this context, combining SCP and AC could represent a promising approach, balancing the sustainability of bio-based materials with the performance reliability of commercial adsorbents. The experimental evidence from this study supports the potential for synergistic effects in mixed formulations.

Future investigations should focus on formulations allowing long-term stable performance of these materials under realistic environmental conditions, including flow dynamics, bioturbation, and contaminant aging.

4. Conclusions

The results of this work demonstrate that SCPs can effectively remove Zn and Cr from seawater. While SCPs exhibited a higher affinity for Cr, the efficiency of Zn removal was more sensitive to initial concentration and the presence of competing ions. The evaluation of SCP/AC mixes revealed that the adsorption efficiency does not always follow a linear trend based on the individual contribution of each adsorbent, showing synergistic effects. These findings highlight the relevance of considering combined systems for optimizing treatment performance. Overall, SCPs emerge as a promising and sustainable adsorbent, offering an innovative approach for metal removal in marine environments while promoting the valorization of agro-industrial by-products from a circular economy perspective.

Author Contributions: Conceptualization, C.M., S.M., A.C. and F.P.; Data curation, C.M.; Formal analysis, C.M.; Funding acquisition, F.P.; Investigation, C.M.; Methodology, C.M.; Project administration, S.M., A.C. and F.P.; Resources, S.M., A.C. and F.P.; Supervision, S.M., A.C. and F.P.; Validation, C.M., S.M. and A.C.; Visualization, C.M.; Writing—original draft, C.M.; Writing—review & editing, C.M., S.M., A.C. and F.P. All authors have read and agreed to the published version of the manuscript.

Funding: This research received no external funding.

Data Availability Statement: The original contributions presented in this study are included in the article. Further inquiries can be directed to the corresponding authors.

Acknowledgments: Chiara Maraviglia would like to thank the Italian Ministry of University and Research (MUR) who provided financial support for her PhD grant in the frame of Mission 4 of Piano Nazionale di Ripresa e Resilienza (PNRR) as regulated by the Ministry Decree 351/2022.

Conflicts of Interest: The authors declare no conflicts of interest.

References

1. Ahamad, M.I.; Yao, Z.; Ren, L.; Zhang, C.; Li, T.; Lu, H.; Mehmood, M.S.; Rehman, A.; Adil, M.; Lu, S.; et al. Impact of heavy metals on aquatic life and human health: A case study of River Ravi Pakistan. *Front. Mar. Sci.* **2024**, *11*, 1374835. [CrossRef]
2. Danovaro, R.; di Montanara, A.C.; Corinaldesi, C.; Dell'anno, A.; Illuminati, S.; Willis, T.J.; Gambi, C. Bioaccumulation and biomagnification of heavy metals in marine micro-predators. *Commun. Biol.* **2023**, *6*, 1206. [CrossRef]
3. Lin, Y.-C.; Chang-Chien, G.-P.; Chiang, P.-C.; Chen, W.-H.; Lin, Y.-C. Multivariate analysis of heavy metal contaminations in seawater and sediments from a heavily industrialized harbor in Southern Taiwan. *Mar. Pollut. Bull.* **2013**, *76*, 266–275. [CrossRef]
4. Peng, W.; Li, X.; Xiao, S.; Fan, W. Review of remediation technologies for sediments contaminated by heavy metals. *J. Soils Sediments* **2018**, *18*, 1701–1719. [CrossRef]
5. Liu, Q.; Jia, Z.; Liu, G.; Li, S.; Hu, J. Assessment of heavy metals remobilization and release risks at the sediment-water interface in estuarine environment. *Mar. Pollut. Bull.* **2023**, *187*, 114517. [CrossRef]
6. Lofrano, G.; Libralato, G.; Minetto, D.; De Gisi, S.; Todaro, F.; Conte, B.; Calabrò, D.; Quatraro, L.; Notarnicola, M. In situ remediation of contaminated marinesediment: An overview. *Environ. Sci. Pollut. Res.* **2017**, *24*, 5189–5206. [CrossRef]
7. Akcil, A.; Erust, C.; Ozdemiroglu, S.; Fonti, V.; Beolchini, F. A review of approaches and techniques used in aquatic contaminated sediments: Metal removal and stabilization by chemical and biotechnological processes. *J. Clean. Prod.* **2015**, *86*, 24–36. [CrossRef]
8. Han, D.; Wu, X.; Li, R.; Tang, X.; Xiao, S.; Scholz, M. Critical Review of Electro-kinetic Remediation of Contaminated Soils and Sediments: Mechanisms, Performances and Technologies. *Water Air Soil Pollut.* **2021**, *232*, 335. [CrossRef]

9. Tabak, H.H.; Lens, P.; van Hullebusch, E.D.; Dejonghe, W. Developments in Bioremediation of Soils and Sediments Polluted with Metals and Radionuclides–1. Microbial Processes and Mechanisms Affecting Bioremediation of Metal Contamination and Influencing Metal Toxicity and Transport. *Rev. Environ. Sci. Biotechnol.* **2005**, *4*, 115–156. [CrossRef]
10. Vandenbossche, M.; Jimenez, M.; Casetta, M.; Traisnel, M. Remediation of Heavy Metals by Biomolecules: A Review. *Crit. Rev. Environ. Sci. Technol.* **2015**, *45*, 1644–1704. [CrossRef]
11. Todaro, F.; Barjoveanu, G.; De Gisi, S.; Teodosiu, C.; Notarnicola, M. Sustainability assessment of reactive capping alternatives for the remediation of contaminated marine sediments. *J. Clean. Prod.* **2021**, *286*, 124946. [CrossRef]
12. Park, S.-J.; Kang, K.; Lee, C.-G.; Choi, J.-W. Remediation of metal-contaminated marine sediments using active capping with limestone, steel slag, and activated carbon: A laboratory experiment. *Environ. Technol.* **2019**, *40*, 3479–3491. [CrossRef]
13. Kutuniva, J.; Mäkinen, J.; Kauppila, T.; Karppinen, A.; Hellsten, S.; Luukkonen, T.; Lassi, U. Geopolymers as active capping materials for in situ remediation of metal(loid)-contaminated lake sediments. *J. Environ. Chem. Eng.* **2019**, *7*, 102852. [CrossRef]
14. Wang, Z.; Song, S.; Wang, H.; Yang, W.; Han, J.; Chen, H. Feasibility of Remediation of Heavy-Metal-Contaminated Marine Dredged Sediments by Active Capping with Enteromorpha Biochar. *Int. J. Environ. Res. Public Health* **2022**, *19*, 4944. [CrossRef]
15. Peydayesh, M.; Mezzenga, R. Protein nanofibrils for next generation sustainable water purification. *Nat. Commun.* **2021**, *12*, 3248. [CrossRef]
16. Rodzik, A.; Pomastowski, P.; Sagandykova, G.N.; Buszewski, B. Interactions of Whey Proteins with Metal Ions. *Int. J. Mol. Sci.* **2020**, *21*, 2156. [CrossRef]
17. Ritala, A.; Häkkinen, S.T.; Toivari, M.; Wiebe, M.G. Single Cell Protein—State-of-the-Art, Industrial Landscape and Patents 2001–2016. *Front. Microbiol.* **2017**, *8*, 2009. [CrossRef] [PubMed]
18. Rao, M.; Varma, A.J.; Deshmukh, S.S. Production of single cell protein, essential amino acids, and xylanase by Penicillium janthinellum. *Bioresources* **2010**, *5*, 2470–2477. [CrossRef]
19. Aggelopoulos, T.; Katsieris, K.; Bekatorou, A.; Pandey, A.; Banat, I.M.; Koutinas, A.A. Solid state fermentation of food waste mixtures for single cell protein, aroma volatiles and fat production. *Food Chem.* **2014**, *145*, 710–716. [CrossRef] [PubMed]
20. Yadav, J.S.S.; Yan, S.; Ajila, C.M.; Bezawada, J.; Tyagi, R.D.; Surampalli, R.Y. Food-grade single-cell protein production, characterization and ultrafiltration recovery of residual fermented whey proteins from whey. *Food Bioprod. Process.* **2016**, *99*, 156–165. [CrossRef]
21. Matassa, S.; Pelagalli, V.; Papirio, S.; Zamalloa, C.; Verstraete, W.; Esposito, G.; Pirozzi, F. Direct nitrogen stripping and upcycling from anaerobic digestate during conversion of cheese whey into single cell protein. *Bioresour. Technol.* **2022**, *358*, 127308. [CrossRef] [PubMed]
22. Pomastowski, P.; Sprynskyy, M.; Buszewski, B. The study of zinc ions binding to casein. *Colloids Surf. B Biointerfaces* **2014**, *120*, 21–27. [CrossRef]
23. Buszewski, B.; Rodzik, A.; Railean-Plugaru, V.; Sprynskyy, M.; Pomastowski, P. A study of zinc ions immobilization by β-lactoglobulin. *Colloids Surf. A Physicochem. Eng. Asp.* **2020**, *591*, 124443. [CrossRef]
24. Peydayesh, M.; Bolisetty, S.; Mohammadi, T.; Mezzenga, R. Assessing the Binding Performance of Amyloid–Carbon Membranes toward Heavy Metal Ions. *Langmuir* **2019**, *35*, 4161–4170. [CrossRef] [PubMed]
25. Ramírez-Rodríguez, L.C.; Barrera, L.E.D.; Quintanilla-Carvajal, M.X.; Mendoza-Castillo, D.I.; Bonilla-Petriciolet, A.; Jiménez-Junca, C. Preparation of a Hybrid Membrane from Whey Protein Fibrils and Activated Carbon to Remove Mercury and Chromium from Water. *Membranes* **2020**, *10*, 386. [CrossRef]
26. Gros, N.; Camões, M.F.; Oliveira, C.; Silva, M.C.R. Ionic composition of seawaters and derived saline solutions determined by ion chromatography and its relation to other water quality parameters. *J. Chromatogr. A* **2008**, *1210*, 92–98. [CrossRef]
27. Handley-Sidhu, S.; Mullan, T.K.; Grail, Q.; Albadarneh, M.; Ohnuki, T.; Macaskie, L.E. Influence of pH, competing ions and salinity on the sorption of strontium and cobalt onto biogenic hydroxyapatite. *Sci. Rep.* **2016**, *6*, 23361. [CrossRef]
28. Kim, R.-Y.; Yoon, J.-K.; Kim, T.-S.; Yang, J.E.; Owens, G.; Kim, K.-R. Bioavailability of heavy metals in soils: Definitions and practical implementation—A critical review. *Environ. Geochem. Heal.* **2015**, *37*, 1041–1061. [CrossRef]
29. Saha, R.; Nandi, R.; Saha, B. Sources and toxicity of hexavalent chromium. *J. Coord. Chem.* **2011**, *64*, 1782–1806. [CrossRef]
30. Knox, A.S.; Paller, M.H.; Roberts, J. Active capping technology—New approaches for in situ remediation of contaminated sediments. *Remediat. J.* **2012**, *22*, 93–117. [CrossRef]
31. Gifuni, L.; de Ruggiero, P.; Cianelli, D.; Zambianchi, E.; Pierini, S. Hydrology and Dynamics in the Gulf of Naples during Spring of 2016: In Situ and Model Data. *J. Mar. Sci. Eng.* **2022**, *10*, 1776. [CrossRef]
32. Tanhua, T.; Hainbucher, D.; Schroeder, K.; Cardin, V.; Álvarez, M.; Civitarese, G. The Mediterranean Sea system: A review and an introduction to the special issue. *Ocean Sci.* **2013**, *9*, 789–803. [CrossRef]
33. Ogata, F.; Kangawa, M.; Iwata, Y.; Ueda, A.; Tanaka, Y.; Kawasaki, N. A Study on the Adsorption of Heavy Metals by Using Raw Wheat Bran Bioadsorbent in Aqueous Solution Phase. *Chem. Pharm. Bull.* **2014**, *62*, 247–253. [CrossRef] [PubMed]
34. Sun, Z.; Tian, C.; Yang, T.; Fu, J.; Xu, H.; Wang, Y.; Lin, Z. A MOF-based trap with strong affinity toward low-concentration heavy metal ions. *Sep. Purif. Technol.* **2022**, *301*, 121946. [CrossRef]

35. Zhang, W.; An, Y.; Li, S.; Liu, Z.; Chen, Z.; Ren, Y.; Wang, S.; Zhang, X.; Wang, X. Enhanced heavy metal removal from an aqueous environment using an eco-friendly and sustainable adsorbent. *Sci. Rep.* **2020**, *10*, 1645. [CrossRef]
36. Kouakou, U.; Ello, A.S.; Yapo, J.A.; Trokourey, A. Adsorption of iron and zinc on commercial activated carbon. *J. Environ. Chem. Ecotoxicol.* **2013**, *5*, 168–171. [CrossRef]
37. Wang, J.; Guo, X. Adsorption isotherm models: Classification, physical meaning, application and solving method. *Chemosphere* **2020**, *258*, 127279. [CrossRef]
38. Zaheer, Z.; AL-Asfar, A.; Aazam, E.S. Adsorption of methyl red on biogenic Ag@Fe nanocomposite adsorbent: Isotherms, kinetics and mechanisms. *J. Mol. Liq.* **2019**, *283*, 287–298. [CrossRef]
39. Wang, C.; Boithias, L.; Ning, Z.; Han, Y.; Sauvage, S.; Sánchez-Pérez, J.-M.; Kuramochi, K.; Hatano, R. Comparison of Langmuir and Freundlich adsorption equations within the SWAT-K model for assessing potassium environmental losses at basin scale. *Agric. Water Manag.* **2017**, *180*, 205–211. [CrossRef]
40. Nieto-Márquez, A.; Pinedo-Flores, A.; Picasso, G.; Atanes, E.; Kou, R.S. Selective adsorption of Pb^{2+}, Cr^{3+} and Cd^{2+} mixtures on activated carbons prepared from waste tires. *J. Environ. Chem. Eng.* **2017**, *5*, 1060–1067. [CrossRef]
41. Amaechi, P.U.; Elenwo, C.E.; Dimkpa, S.O.N. Langmuir and Freundlich Isotherm Models' Description of P. Adsorption Capacity of Wetland and Upland Soil in Rivers State. *Glob. J. Agric. Res.* **2024**, *12*, 14–29. [CrossRef]
42. Nong, Q.; Yuan, K.; Li, Z.; Chen, P.; Huang, Y.; Hu, L.; Jiang, J.; Luan, T.; Chen, B. Bacterial resistance to lead: Chemical basis and environmental relevance. *J. Environ. Sci.* **2019**, *85*, 46–55. [CrossRef]
43. Zamouche, M.; Mouni, L.; Ayachi, A.; Merniz, I. Use of commercial activated carbon for the purification of synthetic water polluted by a pharmaceutical product. *Desalination Water Treat* **2019**, *172*, 86–95. [CrossRef]
44. da Costa Lopes, A.S.; de Carvalho, S.M.L.; do Socorro Barros Brasil, D.; de Alcântara Mendes, R.; Lima, M.O. Surface Modification of Commercial Activated Carbon (CAG) for the Adsorption of Benzene and Toluene. *Am. J. Anal. Chem.* **2015**, *6*, 528–538. [CrossRef]
45. Cardoso, N.F.; Lima, E.C.; Royer, B.; Bach, M.V.; Dotto, G.L.; Pinto, L.A.; Calvete, T. Comparison of Spirulina platensis microalgae and commercial activated carbon as adsorbents for the removal of Reactive Red 120 dye from aqueous effluents. *J. Hazard. Mater.* **2012**, *241–242*, 146–153. [CrossRef]
46. Pet, I.; Sanad, M.N.; Farouz, M.; ElFaham, M.M.; El-Hussein, A.; El-Sadek, M.S.A.; Althobiti, R.A.; Ioanid, A. Review: Recent Developments in the Implementation of Activated Carbon as Heavy Metal Removal Management. *Water Conserv. Sci. Eng.* **2024**, *9*, 62. [CrossRef]
47. Qiao, H.; Qiao, Y.; Luo, X.; Zhao, B.; Cai, Q. Qualitative and quantitative adsorption mechanisms of zinc ions from aqueous solutions onto dead carp derived biochar. *RSC Adv.* **2021**, *11*, 38273–38282. [CrossRef] [PubMed]
48. Liu, J.; Wu, P.; Li, S.; Chen, M.; Cai, W.; Zou, D.; Zhu, N.; Dang, Z. Synergistic deep removal of As(III) and Cd(II) by a calcined multifunctional MgZnFe-CO3 layered double hydroxide: Photooxidation, precipitation and adsorption. *Chemosphere* **2019**, *225*, 115–125. [CrossRef]
49. Ren, X.; Yang, S.; Tan, X.; Chen, C.; Sheng, G.; Wang, X. Mutual effects of copper and phosphate on their interaction with γ-Al2O3: Combined batch macroscopic experiments with DFT calculations. *J. Hazard. Mater.* **2012**, *237–238*, 199–208. [CrossRef] [PubMed]
50. Selvi, K.; Pattabhi, S.; Kadirvelu, K. Removal of Cr(VI) from aqueous solution by adsorption onto activated carbon. *Bioresour. Technol.* **2001**, *80*, 87–89. [CrossRef]
51. Di Natale, F.; Erto, A.; Lancia, A.; Musmarra, D. Experimental and modelling analysis of As(V) ions adsorption on granular activated carbon. *Water Res.* **2008**, *42*, 2007–2016. [CrossRef]
52. Huang, D.; Zhang, Y.; Zhang, J.; Wang, H.; Wang, M.; Wu, C.; Cheng, D.; Chi, Y.; Zhao, Z. The synergetic effect of a structure-engineered mesoporous SiO_2 –ZnO composite for doxycycline adsorption. *RSC Adv.* **2019**, *9*, 38772–38782. [CrossRef]
53. Salah, W.; Djeridi, W.; Houas, A.; Elsellami, L. Synergy between activated carbon and ZnO: A powerful combination for selective adsorption and photocatalytic degradation. *Mater. Adv.* **2024**, *5*, 1667–1675. [CrossRef]
54. Zekavat, S.R.; Raouf, F.; Talesh, S.S.A. Simultaneous adsorption of Cu^{2+} and Cr (VI) using HDTMA-modified zeolite: Isotherm, kinetic, mechanism, and thermodynamic studies. *Water Sci. Technol.* **2020**, *82*, 1808–1824. [CrossRef]
55. Yan, Y.; Wan, B.; Mansor, M.; Wang, X.; Zhang, Q.; Kappler, A.; Feng, X. Co-sorption of metal ions and inorganic anions/organic ligands on environmental minerals: A review. *Sci. Total Environ.* **2022**, *803*, 149918. [CrossRef]
56. Spalvins, K.; Zihare, L.; Blumberga, D. Single cell protein production from waste biomass: Comparison of various industrial by-products. *Energy Procedia* **2018**, *147*, 409–418. [CrossRef]
57. Van Tran, V.; Park, D.; Lee, Y.-C. Hydrogel applications for adsorption of contaminants in water and wastewater treatment. *Environ. Sci. Pollut. Res.* **2018**, *25*, 24569–24599. [CrossRef]
58. Ismail, S.; Giacinti, G.; Raynaud, C.D.; Cameleyre, X.; Alfenore, S.; Guillouet, S.; Gorret, N. Impact of the environmental parameters on single cell protein production and composition by Cupriavidus necator. *J. Biotechnol.* **2024**, *388*, 83–95. [CrossRef] [PubMed]

59. Gęca, M.; Wiśniewska, M.; Nowicki, P. Biochars and activated carbons as adsorbents of inorganic and organic compounds from multicomponent systems—A review. *Adv. Colloid Interface Sci.* **2022**, *305*, 102687. [CrossRef] [PubMed]
60. Cornelissen, G.; Kruså, M.E.; Breedveld, G.D.; Eek, E.; Oen, A.M.; Arp, H.P.H.; Raymond, C.; Samuelsson, G.; Hedman, J.E.; Stokland, Ø.; et al. Remediation of Contaminated Marine Sediment Using Thin-Layer Capping with Activated Carbon—A Field Experiment in Trondheim Harbor, Norway. *Environ. Sci. Technol.* **2011**, *45*, 6110–6116. [CrossRef] [PubMed]
61. Jonker, M.T.O.; Suijkerbuijk, M.P.W.; Schmitt, H.; Sinnige, T.L. Ecotoxicological Effects of Activated Carbon Addition to Sediments. *Environ. Sci. Technol.* **2009**, *43*, 5959–5966. [CrossRef] [PubMed]

Disclaimer/Publisher's Note: The statements, opinions and data contained in all publications are solely those of the individual author(s) and contributor(s) and not of MDPI and/or the editor(s). MDPI and/or the editor(s) disclaim responsibility for any injury to people or property resulting from any ideas, methods, instructions or products referred to in the content.